Supplementary Information

Selective dissolution and re-precipitation by pH cycling enables recovery of manganese from surface nodules

Pravalika Butreddy,[1] Sebastian Mergelsberg,[1] Jennifer N. Jocz,[1] Dongsheng Li,[1] Venkateshkumar Prabhakaran,[1] Andrew J. Ritchhart,[1] Chinmayee V. Subban,[1,2] Jon Kellar,[3] Scott R. Beeler,[4] Sarah W. Keenan,[5]* Elias Nakouzi[1]*

[1] Pacific Northwest National Laboratory, Richland, Washington 99354, United States of America

[2] Department of Materials Science and Engineering, University of Washington, Seattle, Washington 98195, United States of America

[3] Department of Materials and Metallurgical Engineering, South Dakota School of Mines and Technology, Rapid City, South Dakota 57701, United States of America

[4] Engineering and Mining Experiment Station, South Dakota School of Mines and Technology, Rapid City, South Dakota 57701, United States of America

[5] Department of Geology and Geological Engineering, South Dakota School of Mines and Technology, Rapid City, South Dakota 57701, United States of America

***Corresponding Authors**: (SWK) sarah.keenan@sdsmt.edu; (EN) elias.nakouzi@pnnl.gov

Supporting figures

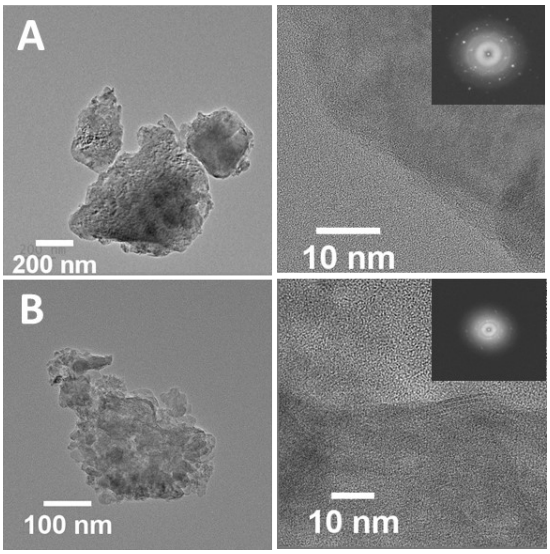

Figure S1. Ex situ TEM image, high-resolution TEM image, and the corresponding diffraction patterns (from left to right) of the pristine Mn nodule powder showing the (A) calcite and (B) siderite.

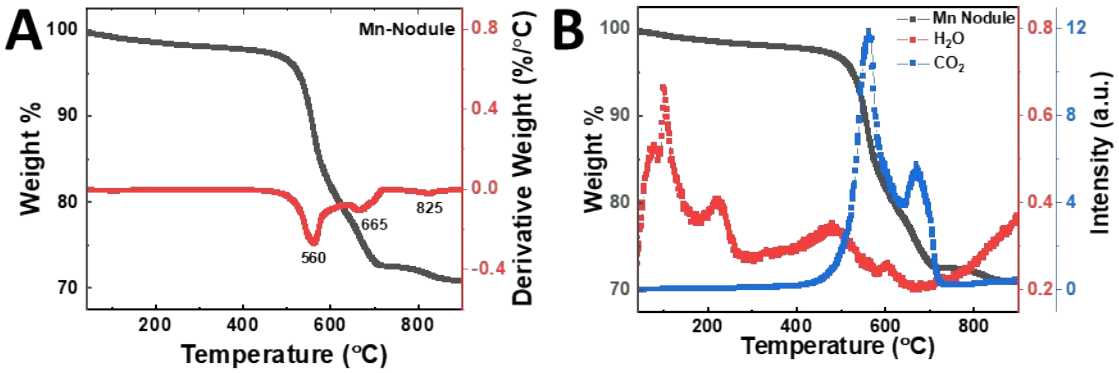

Figure S2. (A) TGA analysis (TA instruments TGA 5500), and (B) Mass spectrometer (MKS Cirrus 3) analysis on the pristine Mn nodule powder (at a ramp rate of 10 °C/min in high-temperature platinum pans). Note: A calcium oxalate monohydrate calibration run was performed before the TGA-MS analysis. In Figure S3A, the peak degradation at 560 °C corresponds to the thermal decomposition of rhodochrosite[1], the mass loss at 665 °C indicates the presence of siderite[2], and the slight degradation peak at 825 °C corresponds to the presence of calcite[3] in the sample. Figure S3B shows the evolution of CO_2 gas from the mass spectrometer in the 500-700 °C range, indicating the presence of carbonates in the pristine Mn nodule powder.

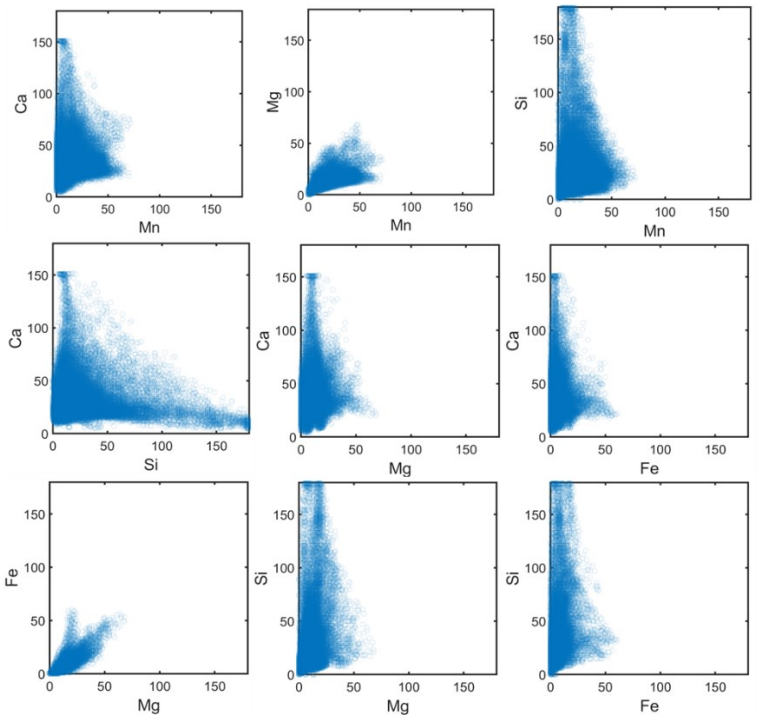

Figure S3. Correlation analysis between various elements

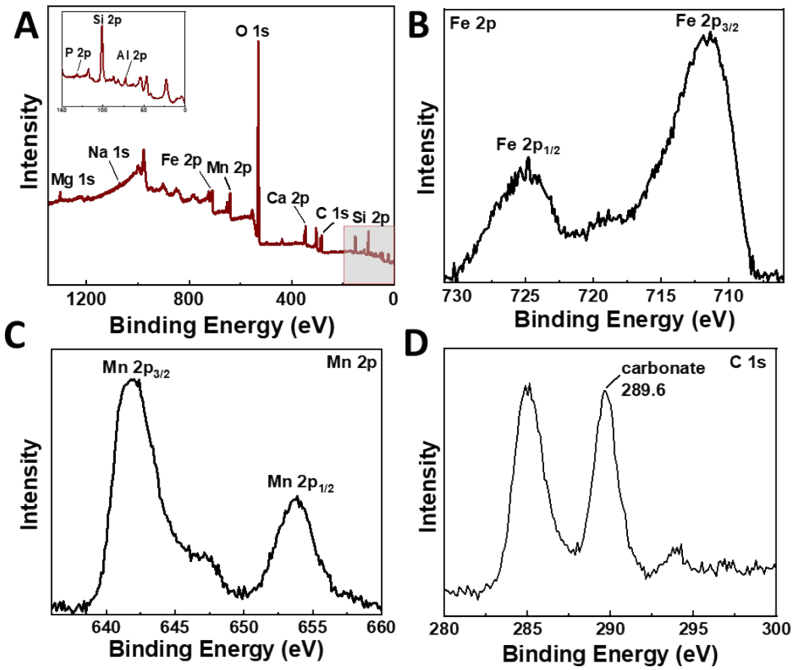

Figure S4. (A) XPS survey spectra and narrow elemental scans of (B) Fe 2p, (C) Mn 2p, and (D) C 1s indicate the presence of carbonates[4-6] in the pristine nodule powder.

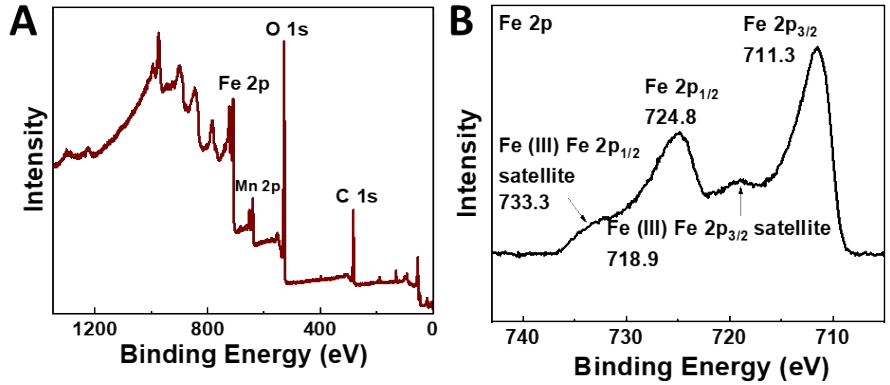

Figure S5. (A) XPS survey spectra and narrow elemental scans of (B) Fe 2p of the pH 5.7 precipitate.

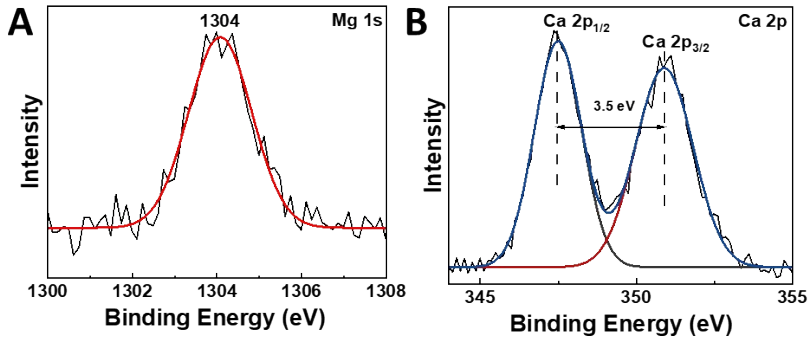

Figure S6. XPS narrow spectra of (A)Mg 1s and (B) Ca 2p of the pH 10.9 precipitate, which shows a peak separation of 3.5eV, indicating the presence of $CaCO_3$.[7]

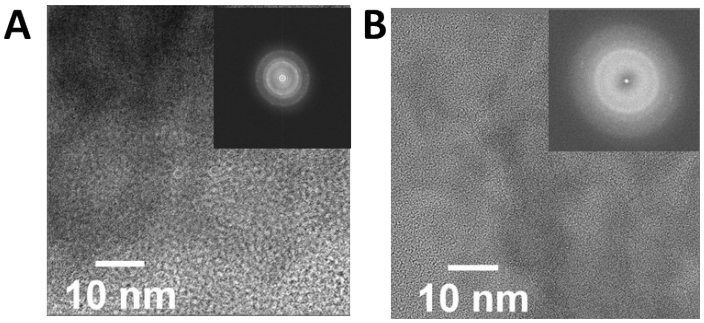

Figure S7. HR-TEM image of the pH 10.9 precipitate showing the (A) Mn_2O_3 and (B) MnO phases.

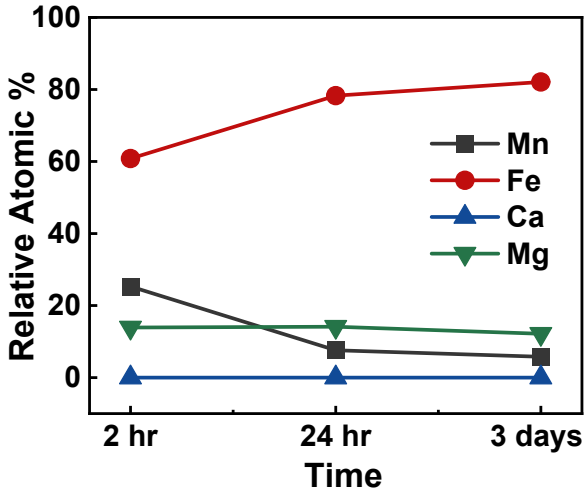

Figure S8. Relative atomic mass of residual powder as a function of leaching time in pH 1.5 solution.

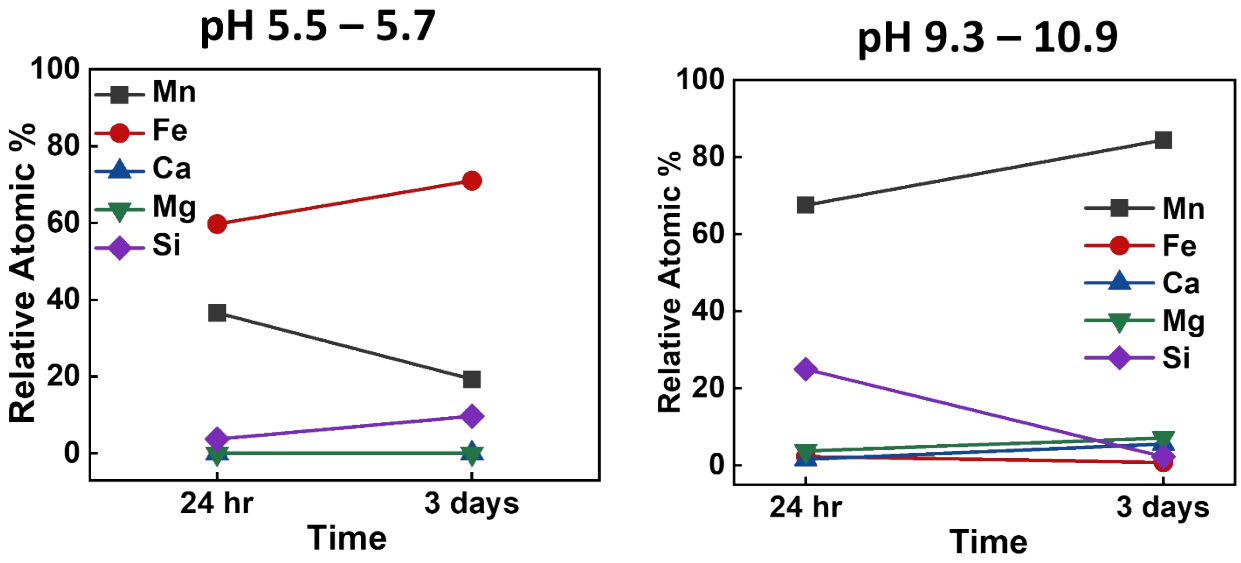

Figure S9. Relative atomic mass of extracted precipitate as a function of leaching time in pH 1.5 solution.

Supporting Tables

	Mn		Fe	Ca	Mg	Na	B	P	Zn	Cr	Cu
Pristine Mn Nodule	214		115.8	100	20.4	38.6	22.8	0	0	1.44	0
pH 5.7 (Fe-rich)	143		588	10	0	44.2	24.2	49.2	0	1.236	2.42
pH 10.9 (Mn-rich)	520		12.8	35	22	45	27	0	1.58	1.58	0

Table S1. Average concentration (ppm) per element from the ICP-OES analysis.

At%	C 1s	O 1s	Na 1s	Mg 2s	Al 2p	Si 2p	P 2p	K 2p	Ca 2p	Mn 2p	Fe 2p
Nodule powder	15.57	58.96	0.30	1.63	1.46	9.66	0.43	0.13	2.96	3.54	5.37
Residue at pH 1.5	8.53	63.19	0.02	0.4	2.46	16.17	0.41	0.25	0.43	0.49	7.65
pH 5.7	29.06	46.22	0.08	0.05	0.20	0.31	2.01	-	-	3.82	18.25
pH 10.9	8.03	57.93	0.17	3.28	0.16	0.53	-	-	2.8	26.81	0.28

Table S2. Atomic concentration table acquired from the survey scans using XPS analysis on the pristine nodule powder, precipitates at pH 5.7 and pH 10.9, and manganese nodule residue at pH 1.5.

Wt%	C 1s	O 1s	Na 1s	Mg 2s	Al 2p	Si 2p	P 2p	K 2p	Ca 2p	Mn 2p	Fe 2p
Nodule powder	8.83	44.53	0.32	1.87	1.86	12.81	0.62	0.24	5.6	9.17	14.16
Residue at pH 1.5	4.79	47.29	0.02	0.45	3.11	21.25	0.59	0.46	0.8	1.26	19.97
pH 5.7	14.56	30.85	0.07	0.06	0.23	0.37	2.6	-	-	8.75	42.52
pH 10.9	3.54	33.99	0.15	2.92	0.16	0.54	-	-	4.12	54.02	0.58

Table S3. Weight percentage table acquired from the survey scans using XPS analysis on the pristine nodule powder, precipitates at pH 5.7 and pH 10.9, and manganese nodule residue at pH 1.5.

Estimation of manganese recovery rate from EDS and ICP-OES measurements

Element	Concentration (ppm)	Relative mass	molar mass of metal element/ molar mass of mass of compound	mass of compound	% mass of compound	mass of compound in recovered 5.6 mg	milligrams of element
Mn	520.00	0.82	1.58	1.29	0.78	4.39	2.78
Fe	12.80	0.02	1.91	0.04	0.02	0.13	0.07
Ca	35.00	0.05	1.85	0.10	0.06	0.35	0.19
Mg	22.00	0.03	2.40	0.08	0.05	0.28	0.12
Na	45.00	0.07	1.74	0.12	0.07	0.42	0.24
Cr	1.58	0.00	1.98	0.00	0.00	0.02	0.01
Zn	1.58	0.00	1.51	0.00	0.00	0.01	0.01

Table S4. Workflow to estimate manganese recovery rate using ICP-OES data. Mn element assumed to exist as MnO_2, the other metals are assumed to exist as hydroxides.

Element	Weight %	Relative mass	molar mass of metal / molar mass of mass of compound	mass of compound	% mass of compound	mass of compound in recovered 5.6 mg	milligrams of element
Mn	59.20	0.91	1.58	1.44	0.89	4.97	3.15
Fe	0.50	0.01	1.91	0.01	0.01	0.05	0.03
Ca	2.80	0.04	1.85	0.08	0.05	0.28	0.15
Mg	1.80	0.03	2.40	0.07	0.04	0.23	0.10
Na	0.60	0.01	1.74	0.02	0.01	0.06	0.03
Al	0.10	0.00	2.90	0.00	0.00	0.02	0.01

Table S5. Workflow to estimate manganese recovery rate using EDS data. Mn element assumed to exist as MnO_2, the other metals are assumed to exist as hydroxides.

REFERENCES

1. Z. Tu, X. Liang, C. Wu and Y. Wang, *Journal of Thermal Analysis and Calorimetry*, 2022, **147**, 6481-6488.
2. D. Alkaç and Ü. Atalay, *International Journal of Mineral Processing*, 2008, **87**, 120-128.
3. T. Siva, S. Muralidharan, S. Sathiyanarayanan, E. Manikandan and M. Jayachandran, *Journal of Inorganic and Organometallic Polymers and Materials*, 2017, **27**, 770-778.
4. M. P. Casaletto and G. Fierro, *Applied Surface Science*, 2017, **421**, 97-108.

5. B. Xing, N. Graham and W. Yu, *Communications Chemistry*, 2020, **3**, 38.
6. P. G. Rouxhet and M. J. Genet, *Surf Interface Anal*, 2011, **43**, 1453-1470.
7. Q. Liu, J. Li, Z. Zhou, J. Xie and J. Y. Lee, *Scientific Reports*, 2016, **6**, 19593.